Electronic Structure of Transition Metals. I. Quantum Defects and Model Potential*

A. O. E. Animalu
Lincoln Laboratory, Massachusetts Institute of Technology, Lexington, Massachusetts 02173
(Received 5 February 1973)

Recent applications of the concept of quantum defects in setting up model pseudopotentials for simple or transition-metal ions presuppose that the atomic-spectroscopy data of such metals can be expressed in terms of certain quantum defects. **Experience indicates, however, that the old quantum-defect idea applies only to group I and II metals at best, but not to metals of higher chemical valence ($z \geq 3$, z being the nominal valence given by the group number, I*A* or *B*, II*A* or *B*, etc. in the Periodic Table). In this paper, a generalized quantum-defect law applicable to elements having $z \geq 2$ is deduced empirically from an extensive study of the spectroscopic data of the first six rows of the Periodic Table. The empirical law states that the energy levels E_{nl} of a single electron in the field of the positive ions of elements having the same inert-gas core, e.g., the elements of the isoelectric sequence, Li^+, Be^{2+}, ... ,F^{7+}, which are given (in the Heine-Abarenkov model-potential method) by the spectroscopic term value of the ion *plus* one electron, i.e., by the term values of Li, Be^+, ··· ,F^{6+},** by the term values of Li, Be^+, ···, F^{7+}, obey the relation $E_{nl} = -z^2/(n-\delta_{nl})^2 + \Delta_{nl}$, $z \geq 2$, for the *same* quantum defects (δ_{nl}, Δ_{nl}). The old quantum defect (δ_{nl}) and the new quantum defect (Δ_{nl}, equivalent to an "atomic core shift") thus represent the deviation of the atomic potential of a given inert-gas configuration from a Coulombic potential due to a nuclear charge $z|e|$. On the basis of this empirical law, the parameters of a transition-metal model potential of the Heine-Abarenkov type, adjusted to the energies $\mathcal{E}_{nl} \equiv E_{nl} - \Delta_{nl}$, have been calculated for all 30 group-*B* (excepting rare-earth) metals of the Periodic Table; and it has been found that the $l = 2$ model potential parameter A_2 reflects the Ziman-Heine-Hubbard resonance model of *s*-*d* hybridization through its strong energy dependence of the form $(\mathcal{E} - \mathcal{E}_{3d})^{-1}$ for the 3*d* series, and similarly for the 4*d* and 5*d* series. The application of the new model potential to the calculation of the various aspects of the electronic structure of solids will be presented in the next and subsequent papers of this series.

I. INTRODUCTION

In this and subsequent articles,[1] the electronic structure of the transition metals will be studied in the pseudopotential approximation based on a new transition-metal model potential (TMMP) of the Heine-Abarenkov type[2-4]:

$$V_m = -\sum_l A_l P_l \quad \text{for} \quad r \leq R_m$$
$$= -z/r \quad \text{for} \quad r > R_m. \tag{1}$$

The symbols have their usual meaning: P_l is the projection operator that picks out the lth angular-momentum component of an incident one-electron wave function, A_l (which depends on l as well as on energy E) is a parameter representing the depth of a potential well for given model radius R_m, and z is the chemical valence of the isolated ion of the metal. The TMMP represents the bare (unscreened) electron-ion-interaction potential energy at a separation r, and has to be screened by the dielectric constant of the valence-electron gas in order to obtain the effective (screened) or self-consistent potential seen by a single valence electron in the metal.

In extending the model-potential method to the transition metals, several questions arise. The model potential parameters A_l are to be determined at the observed atomic-spectroscopic term values[5] E_{nl} for the isolated ion or atom and extrapolated to the appropriate energy, say E_F, of the electron at the Fermi level in the solid in the spirit of the quantum-defect method[6] (QDM). Thus, in the first place, the quantum-defect concept should be extended to the transition metals, which is the problem tackled in this paper of the series. The next basic question concerns the screening of the TMMP and the application of the screened TMMP form factors $V(q)$ to calculation of solid-state properties: we choose for this purpose the calculation of the phonon spectrum of the transition metals which will be presented in Paper II of the series.[1] Finally, the question of electronic energy-band structure and the characterization of *s*-*d* hybridization will be discussed in Paper III. Each question will be introduced more fully in respective Papers I, II, and III.

It should be stressed that although our primary interest is the transition metals, the present study has been motivated by the systematics of the spectroscopic data of 56 elements, including both simple (mostly group *A*) and the transition (excepting the rare-earth) metals. The spectroscopic data indicate that the relevant factor correlating the behavior of elements along a given row of the Periodic Table is the common inert-gas structure of the ion cores as well as the *chemical valence* (z), and hence the atomic number. As a result, most physical properties turn out to depend on z in a simple way for elements characterized by the same inert-

gas core: unfortunately, z varies considerably for the transition metals and we have had to use the chemistry of the transition-metal ions and other empirical data to choose this important parameter of the TMMP.

We now turn to introduce the quantum-defect question more fully in the context of the Heine-Abarenkov (HA) method. Even for the simple metals, the HA prescription[2,3] for applying the QDM raises the question: does the concept of quantum defect apply to all nontransition (group-A) elements of the Periodic Table, and if so in what form? The failure to answer this question first, before the model-potential calculations of Animalu and Heine,[4] meant that the extrapolation of model-potential parameters in the spirit of the QDM remained an undefined concept. The question became exacerbated the more in earlier attempts[7] to extend the HA method to the transition metals: does the concept of quantum defect apply to both simple (group A) and the transition (group-B) metals of the Periodic Table? It is true, however, that a solution of the problem for the simple metals was eventually found empirically[8] by looking at the spectroscopic term values of over 30 elements of the Periodic Table: the solution was that if $R_m \simeq R_c$ (the ion-core radius), a linear extrapolation of A_l as a function of the energy E is satisfactory, except (as pointed out later by Shaw[9]) for d-shell electron-energy levels. But the reason for this has remained obscure to date, and as a result a natural extension of the HA method to the transition metals could not be founded on familiar grounds.

The aim of this paper therefore is to answer this basic question first and (because the answer turns out to be simple) then extend the HA method to the transition metals. The basic question of extending the concept of quantum defect to all elements of the Periodic Table can be phrased somewhat more directly as follows: how seriously does the potential of an electron in the neighborhood of an isolated positive ion of an element, in particular a transition metal, differ from a Coulomb potential due to a nuclear charge $z|e|$? Since the QDM is expected to work only if the potential eventually becomes Coulombic within a Wigner-Seitz atomic sphere of radius $R_a > R_c$, so that a model radius R_m can be found in the range $R_c \leq R_m < R_a$, the question boils down to one of estimating the size of the ion core R_c in relation to R_a.

According to Harrison,[10] it is the small-core approximation ($R_c/R_a \simeq 0.5$ for K^+, a simple metal ion) which breaks down for transition metals ($R_c/R_a \simeq 1$, for Cu^+, a typical group-B metal, according to the estimate based on the renormalized-atom method of Hodges, Watson, and Ehrenreich[11]). These theoretical estimates of R_c in transition metals are, however, at variance with the empirical Pauling radius[12] ($R_c/R_a = 0.41$ for K^+, $R_c/R_a = 0.54$ for Cu^+), on which the model potentials[1,4] are based. In other words, while the renormalized-atom method[11] suggests that the atomic potential hardly becomes Coulombic inside the Wigner-Seitz sphere for transition metals, empirical Pauling radii suggest that the deviation from Coulombic behavior must be of a simple nature.

A way of obtaining experimental evidence, for or against the *large-core model*[10,11] of transition metals, is to examine the accuracy of the quantum-defect concept when applied to the transition metals. To the best of our knowledge, no previous application of the QDM to the transition metals exists in current literature: the most recent effort by Seaton[13] had led to an extension of the QDM to divalent metals, for atomic scattering rather than solid-state applications. It is therefore to be expected that a successful extension of the quantum-defect concept to the transition metals will be of interest in solid-state physics, atomic physics and chemistry. Such an extension will be presented in Sec. II.

The outline of the rest of this paper is as follows. The application of the extension of the quantum-defect concept to the construction of the transition-metal model potential will be discussed in Sec. III. Numerical results will be presented in Sec. IV and conclusions will be drawn in Sec. V.

II. QUANTUM-DEFECT LAW FOR ELEMENTS OF ISOELECTRONIC SEQUENCE

The concept of quantum defect was introduced for central potentials in the early days of atomic-structure calculations by Hartree,[14] and has been used since then to explore solid-state properties (as the QDM[6]), and more recently autoionization cross sections[13] in atomic physics. The essence of the concept is to utilize the spherical symmetry of an atom in exhibiting the close resemblance of the optical spectra of the alkali metals and the spectra of hydrogen atom: Since the alkali metals and hydrogen belong to the same *column* (group IA) of the Periodic Table, and the positive ions of the alkali metals, Li^+, Na^+, K^+, etc., are simulated by H^+ closely, the resemblance in question correlates the elements on the basis of their common chemical valence ($z = 1$).

In this section, we shall try instead to correlate elements along a *row* of the Periodic Table in the spirit of Moseley's law as applied to an isoelectronic sequence by Bowsen and Millikan.[15] The motivation, physically, is that a valence electron outside an inert-gas shell (characterizing a row of the Periodic Table) tends to be kept out from the core by the Pauli exclusion principle and will therefore feel a Coulombic potential due to a nuclear charge $z|e|$ having the same configurational dis-

tribution along a row of the Periodic Table. To be explicit, we shall bear in mind two isoelectronic sequences of simple and transition metals: these are the second-row sequence,

$$Li^{+},\ Be^{2+},\ B^{3+},\ C^{4+},\ N^{5+},\ O^{6+},\ F^{7+} \tag{2}$$

and the Group-B elements of the fourth row,

$$Cu^{+},\ Zn^{2+},\ Sc^{3+},\ Ti^{4+},\ V^{5+},\ Cr^{6+},\ Mn^{7+},$$

$$Fe^{8+},\ Co^{9+},\ Ni^{10+}. \tag{3}$$

It should be observed, however, that Cu^{+} and Zn^{2+} have the configurations $1s^2\,2s^2\,2p^6\,3s^2\,3p^6\,3d^{10}$, whereas Sc^{3+}, Ti^{4+}, ..., Ni^{10+} have the configuration $1s^2\,2s^2\,2p^6\,3s^2\,3p^6$, i.e., have ten electrons *less* than Cu^{+} and Zn^{2+}. Thus, Cu^{+} and Zn^{2+} do not, according to our definition of isoelectronic sequence, belong to the sequence of Eq. (3); instead, K^{+} and Ca^{2+} (in the same row of the Periodic Table), which are simple metals, do belong to the sequence of Eq. (3), while Cu^{+} and Zn^{2+} logically belong to Ga^{3+}, Ge^{4+}, As^{5+}, Se^{6+}, Br^{7+} isoelectronic sequence. We shall return to this point in the last few paragraphs of Sec. III.

Now, because of the spherical symmetry of an atom, the spectroscopic term values can be labeled by the usual quantum numbers (n, l, m) of the hydrogen atom. In the case of spin doublets, a weighted mean of the two levels may be used to characterize a state of pure l. For an electron moving in an attractive Coulomb potential $-z/r$, the energy levels are

$$E_n = -z^2/n^2\ (\mathrm{Ry}),$$

where n is an integer that increases by unity between adjacent terms of the same series. [We shall work throughout in atomic units $e=\hbar=m=1$, but E_n will be expressed in rydbergs, so that $\frac{1}{2}E_n$ is the energy expressed in the atomic units (hartrees)].

For a modified central potential $V(r)$ which tends to the form $-z/r$ for large r, the eigenvalues may be expressed in terms of an effective quantum number N:

$$E_n = -z^2/N^2 \equiv -z^2/(n-\delta_n)^2. \tag{4}$$

The parameter

$$\delta_n = n - N, \tag{5}$$

called the quantum defect, provides a measure of the difference between $V(r)$ and the Coulomb potential $-z/r$. But, as is well known, this works perfectly well only for the alkali metals (for $z=1$). (The quantum defects are slowly varying functions of energy: a fact on which the success of the QDM depends.) However, for complex atoms having more than one valence electron ($z=2, 3, \ldots$) outside the inert-gas closed shell, the spectra become bewilderingly complicated and the quantum defect seems no longer to work. The presence of more than one electron outside the inert-gas shell introduces exchange and correlation effects causing $V(r)$ to deviate appreciably from a central potential. There is no systematic way of seeing how the quantum defect is modified by this. But we have found in the course of the present attempt to extend the model-potential method to the transition metals that the required modification is as follows:

$$E_{nl} = -z^2/(n-\delta_{nl})^2 + \Delta_{nl}. \tag{6}$$

Here E_{nl} is the energy level of a single electron in the field of a positive ion, such as Be^{2+}, which (in model-potential theory[2-4]) is given by the spectroscopic-term values of the positive ion plus one electron, i.e., by the term values of Be^{+}. δ_{nl} is the old quantum defect and Δ_{nl} a new quantum defect, which may be interpreted as an "atomic" core shift, because of its connection with the Lin-Phillips core shift of pseudopotential theory[16]: the two quantum defects have the remarkable property that they are separately the *same* for fixed (n, l) for a given inert-gas configuration, i.e., for positive ions of an isoelectronic sequence, such as (2) and (3), for $z \geq 2$.

The impressive accuracy of the generalized quantum-defect law (6) is exhibited in Figs. 1(a) and 1(b), for the isoelectronic sequences (2) and (3), using the observed spectroscopic data.[5] Basically, Eq. (6) asserts that a plot of E_{nl} versus the valence z^2 will be *linear*, with a slope determining δ_{nl} and an intercept on E axis determining Δ_{nl}. Unfortunately, Moore's atomic-energy levels[5] are incomplete, and so it is not possible at this time to test the validity of the empirical law (6) for Co^{9+} and Ni^{10+}: However, the fact that Fe^{8+} fits the scheme rather well suggests that (6) may be used to predict the expected values of the spectroscopic-term values of Co^{9+} and Ni^{10+}. The possibility of predicting yet unobserved spectroscopic-term values with the aid of (6) is perhaps the most important consequence of the relation. Observe that, in general, Δ_{nl} is small $\simeq -\frac{1}{2}$ Ry: If it is neglected, then E_{nl} will scale with z^2 in the same way that the original Rydberg formula scales with the atomic number Z^2. We believe that Eq. (6) is new.

III. TRANSITION-METAL MODEL POTENTIAL FOR POSITIVE IONS

We next turn to the question of setting up a model potential V_m, defined by Eq. (1), to simulate the information contained in the quantum defects (δ_{nl}, Δ_{nl}) about the nature of the true atomic potential $V(r)$. In view of the fact that Δ_{nl} represents a shift of the zero of energy E_{nl} for a given set of quantum numbers (n, l) describing the state of a single electron in the field of a positive ion, it is apparent that the QDM should refer to only the Coulombic part of the true potential. Accordingly, we may write

the true one-electron atomic potential for the electronic state (n, l) as

$$V_{nl}(r) = \tilde{V}_{nl}(r) + \tfrac{1}{2}\Delta_{nl} \text{ (a.u.)} \tag{7}$$

and the true radial wave equation as

$$\left(-\frac{\frac{1}{2}d^2}{dr^2} + \frac{l(l+1)}{2r^2} + \tilde{V}_{nl}(r)\right)P_{nl}(r) = \tfrac{1}{2}(E_{nl} - \Delta_{nl})P_{nl}(r)\,, \tag{8}$$

where $\tilde{V}_{nl}$ is Coulombic for r greater than R_c (the ion-core radius). It is the potential $\tilde{V}_{nl}$ that we wish to represent by the model potential (1), so as to reproduce the eigenvalue $\mathcal{E}_{nl} \equiv E_{nl} - \Delta_{nl}$ exactly, within the framework of pseudopotential theory and QDM.

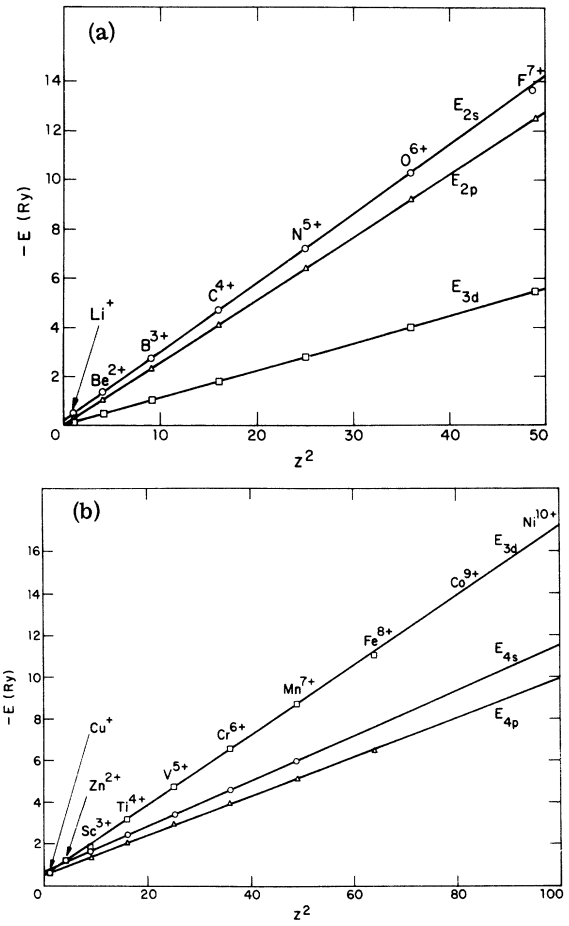

FIG. 1. Spectroscopic term values E_{nl} [of Eq. (6)] as function of the square (z^2) of the chemical valence (a) for the isoelectronic sequence of Eq. (2), and (b) for the isoelectronic sequency of Eq. (3). E_{nl} for Be^{2+}, say, is obtained from the term values[5] of Be^+ (called Be II in Ref. 5) and expressed in Ry, using 109737.3 $cm^{-1} = 1$ Ry, relative to the spectroscopic limit (E_{2s}); E_{2p} is the weighted mean, $\frac{1}{3}(E_{2p(1/2)} + 2E_{2p(3/2)})$ of the doublet E_{nl}; with total spin $j = l \pm \frac{1}{2}(l = 1)$; and similarly for E_{3d}. Open circles, triangles, and squares represent observed term values for s, p, and d levels, respectively.

The model potential for a positive-transition metal ion, for a given angular-momentum state is thus [at arbitrary energy, $\mathcal{E} \equiv E - \Delta$ (Ry)]

$$V_m^l = -A_l(\mathcal{E}) \quad \text{for} \quad r \leq R_m$$
$$= -z/r \quad \text{for} \quad r > R_m, \tag{9}$$

in atomic units. The model wave function for the lth angular-momentum state on which it acts (in an isolated atom or ion) is of the form

$$\phi_l = [\chi(r)/r]Y_{lm}(\theta, \varphi)$$

and the model radial-wave equation is

$$\left(-\frac{\frac{1}{2}d^2}{dr^2} + \frac{l(l+1)}{2r^2} + V_m^l\right)\chi(r) = \tfrac{1}{2}\mathcal{E}\chi(r)\,. \tag{10}$$

Under the *scale transformation*

$$r \to \rho = zr, \quad \mathcal{E} \to \mathcal{E}' = \mathcal{E}/z^2, \tag{11}$$

Eq. (10) reduces, for $r > R_m$, to the radial-wave equation for a hydrogenic atom of effective nuclear charge $z = 1$. As a result, A_l/z^2 is a function of the reduced energy $\mathcal{E}'$ at the scaled-model radius zR_m, and is the same for *all* elements of an isoelectric sequence, such as those in Eqs. (2) and (3), at the equivalent atomic-term values $\mathcal{E}'_{nl}$. This is a consequence of the generalized quantum defect law of Eq. (6).

Given this model, the determination of the model-potential parameters becomes equivalent to that outlined by Heine and Abarenkov[2]: we treat Eq. (10) as an eigenvalue equation for $\mathcal{E}$, if A_l is known at given R_m, or conversely, as an eigenvalue equation for A_l at given R_m for values of $\mathcal{E}$ equal to the appropriate spectroscopic-term value of the free atom or ion. As a matter of fact, the three parameters, A_l, $\mathcal{E}$, and R_m are *not* independent: if we define the variable

$$X = R_m(2A_l - |\mathcal{E}|)^{1/2} \equiv (zR_m)(2A_l/z^2 - |\mathcal{E}|/z^2)^{1/2}\,, \tag{12}$$

then it is readily shown [Ref. 2, Eq. (16)] by matching the *logarithmic derivatives*, χ'/χ of the interior solution ($r \leq R_m$) and the exterior solution ($r > R_m$) of Eq. (10) that one obtains an eigenvalue problem for X,

$$\frac{Xj_{l-1}(X)}{j_l(X)} - l = \frac{{}^0D^l(zR_m) + \gamma(N, l)\,{}^1D^l(zR_m)}{{}^0U^l(zR_m) + \gamma(N, l)\,{}^1U^l(zR_m)}\,. \tag{13}$$

Here, the functions ${}^0U^l$ and ${}^1U^l$ are the Coulomb wave functions (tabulated by Blume *et al.*[17]) which are, respectively, regular and irregular at the origin; their respective derivatives (also tabulated in Ref. 17) are the ${}^0D^l$ and ${}^1D^l$, where $D^l = \rho(dU^l/d\rho)$; and the $j_l(X)$ are spherical Bessel functions which can be written in terms of sines and cosines. The ratio $\gamma(N, l)$ of the two Coulomb wave functions is the usual one that involves the quantum defect (δ_{nl}) via the effective quantum number $N \equiv n - \delta_{nl}$, in the

QDM (Ref. 6, pp. 147–149):

$$\gamma(N,\, l)=\frac{\Gamma(N-l)\tan\pi(N-l-1)N^{2l+1}}{\Gamma(N+l+1)}\,. \qquad (14)$$

The ratio gives the appropriate linear combination of the Coulomb wave functions which decays exponentially at infinity (at atomic-term values $\mathcal{E}_{nl}$).

The numerical solution of Eq. (13) is quite tedious,[2,8] but the results have simple limiting values that can be readily understood, viz., when R_m falls at a turning point, so that $\chi'(R_m)=0$, and when R_m falls at a radial mode, so that $\chi(R_m)=0$. In the first situation, Eq. (13) reduces for $l=0$ to

$$X\cot X=0\,,$$

which has an obvious solution $X=0$, and hence by virtue of Eq. (12),

$$A_0=\tfrac{1}{2}\,|\,\mathcal{E}\,|\,. \qquad (15)$$

This simple result asserts that A_0 will have the same dependence on z^2 as the spectroscopic term values $\mathcal{E}_{nl}$ for elements of an isoelectronic sequence independent of the value of R_m satisfying $\chi'(R_m)=0$. It is apparent from Fig. 2 showing E_{nl} vs z^2 [Fig. 2(a)] and A_l vs z^2 [Fig. 2(b)], based on the model-potential parameters for the nontransition metals

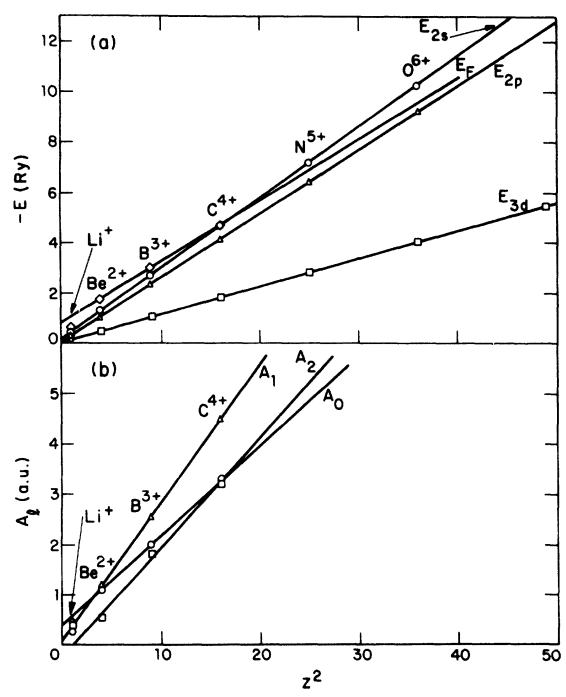

FIG. 2. (a) E_{nl} vs z^2 is the same as in Fig. 1(a), but also shown is the Fermi energy E_F of an electron relative to an ion [as calculated in Ref. 8, using Eq. (23) of Ref. 4 and experimental data]. (b) Model potential parameters A_l vs z^2 at E_F for the R_m's of Ref. 4 (Table 4) and Ref. 18 (Table 1); observe that $zR_m=2.8$ for Li, 4.0 for Be, and 6.0 for B and C [see Eq. (11)].

(Ref. 4, Table 4 and Ref. 18, Table 1) at $E=E_F$, that the proportionality of A_l to $\mathcal{E}$ in Eq. (15) is close to the physical situation in a crystal. It should be recalled that in Refs. 4 and 18, R_m has been chosen for the nontransition metals so that the model wave function has no radial node in the region $r<R_m$ (a condition that was easily fulfilled in the computer programs[8]) which is tantamount to choosing R_m close to the first turning point of the model wave function, usually outside R_c.

In the second situation, such that $\chi(R_m)=0$, the logarithmic derivative χ'/χ becomes infinite and hence, for $l=0$, Eq. (13) reduces to $\sin X=0$. The roots are $X_n=n\pi$, n being an integer (or zero), and hence by virtue of Eq. (12),

$$A_0=\tfrac{1}{2}\,|\,\mathcal{E}\,|+\tfrac{1}{2}(n\pi/R_m)^2\,. \qquad (16)$$

In this situation, A_0 vs z^2 will again be linear for elements of an isoelectronic sequence and have a nonzero intercept on the A axis that depends on R_m. As a result, if R_m is exactly the same for all elements of such a sequence, the linearity of A_l vs z^2 will be maintained.

It is also valuable to establish a general condition for the model potential to be continuous ($A_l=z/R_m$). Suppose that $X_\lambda=z\lambda$ is any eigenvalue of Eq. (13). Then, by virtue of Eq. (12), we must have

$$A_l=\tfrac{1}{2}\,|\,\mathcal{E}\,|+\tfrac{1}{2}(\lambda z/R_m)^2\,. \qquad (17)$$

Thus, if A_l is to be equal to z/R_m, then we should satisfy the quadratic equation

$$\lambda^2(z/R_m)^2-2(z/R_m)+|\,\mathcal{E}\,|=0\,.$$

Naturally, we demand that this equation should have only one root; this is the case if $\lambda^2\mathcal{E}=1$, and the common root is $z/R_m=|\,\mathcal{E}\,|\,(=A_l)$. In short, the depth of the model-potential well A_l (measured in atomic units) has to be numerically equal to the magnitude of the electron energy $\mathcal{E}$ (measured in Ry).

Turning now to the results of numerical solution of Eq. (13) tabulated by Abarenkov[2] (Fig. 3), we see, in addition, that $A_l(\mathcal{E})$ may become *infinite* at some atomic-term values, $\mathcal{E}_{nl}$. Figure 3(a) shows Abarenkov's A_l vs $\mathcal{E}$ for $l=0$, 1, 2 and the spectroscopic term values of Cu (appropriate for the model potential of Cu^+), viz., the 4*s*, 5*s*, 6*s*; 4*p*, 5*p*, 6*p*; and 3*d* [estimated from Eq. (6)], 4*d*, 5*d*, for the *actual* values of $E_{nl}\equiv\mathcal{E}_{nl}+\Delta_{nl}$. In this plot, we see that A_0 and A_1 vary smoothly with energy through the atomic-term values, while A_2 goes through infinity at E_{4d} and E_{5d}, but not at the expected position of the *d*-band resonance, E_{3d}. However, as we have pointed out, we should really set up a model potential for the "core-shifted energies," $\mathcal{E}_{nl}$ (rather than the actual E_{nl}); if this is done, using the fact that $-\Delta_{3d}\simeq\frac{1}{2}$ (Ry) [from Fig. 1(b)] $\simeq E_{4d}-E_{3d}$ (from spectroscopic data[5]) i.e., $\mathcal{E}_{3d}\simeq E_{4d}$, then the net

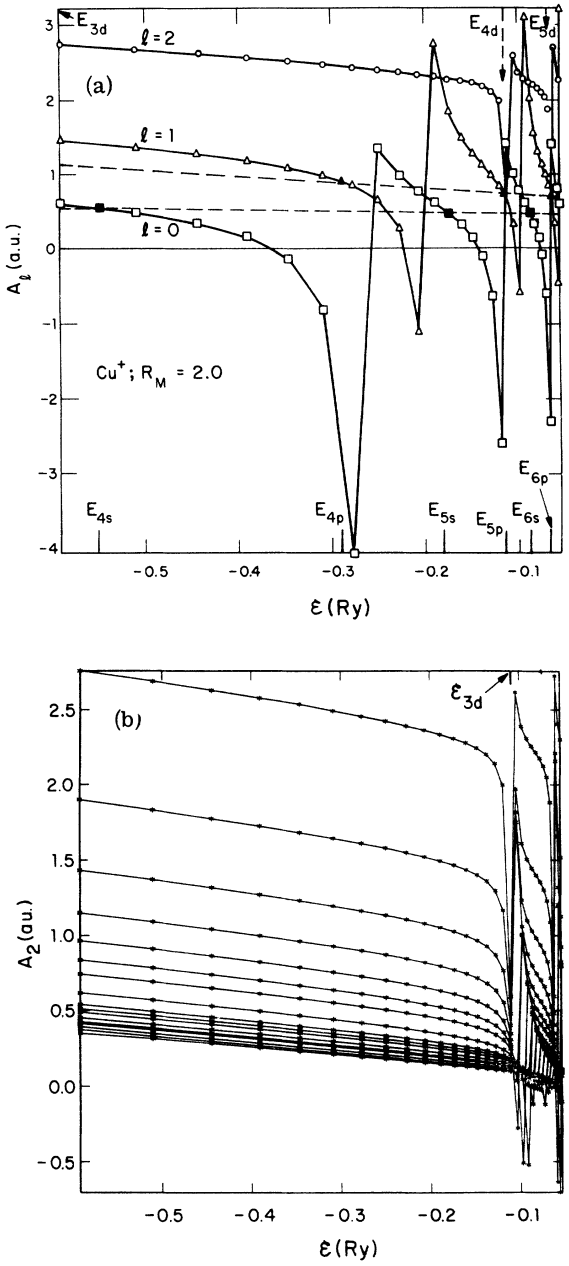

FIG. 3. (a) Abarenkov's tables[2] (in graphical form) for the model-potential parameters $A_l (l = 0, 1, 2)$ for $R_m = 2.0$ (a.u.) and $z = 1$ for Cu^+, as function of arbitrary energy parameter $\mathcal{E}$. The positions of the actual spectroscopic-term values E_{4s}, E_{5s}, E_{6s}; E_{4p}, E_{5p}, E_{6p}; E_{3d} [based on Fig. 1(b)], E_{4d}, E_{5d}, are indicated on the horizontal scale. The dashed lines for $l = 0$, 1 represent the linear A_l-vs-$\mathcal{E}$ relation previously used for the nontransition metals in Ref. 8. Observe that E_{4d} (rather than E_{3d}) as well as E_{5d} fall at the point where A_2 goes through infinity: when corrected for "core shift," one finds $\mathcal{E}_{3d} \simeq E_{4d}$ and $\mathcal{E}_{4d} \simeq E_{5d}$, i.e., the infinity occurs at the right position $\mathcal{E}_{3d}$. (b) A_2 vs $\mathcal{E}$ (for $z = 1$) for all values of R_m tabulated by Abarenkov (Ref. 2), indicating the immobility of the infinity at $\mathcal{E}_{3d}$ as R_m varies. The infinity simulates the d-band resonance model, empirically [see Eq. (18)].

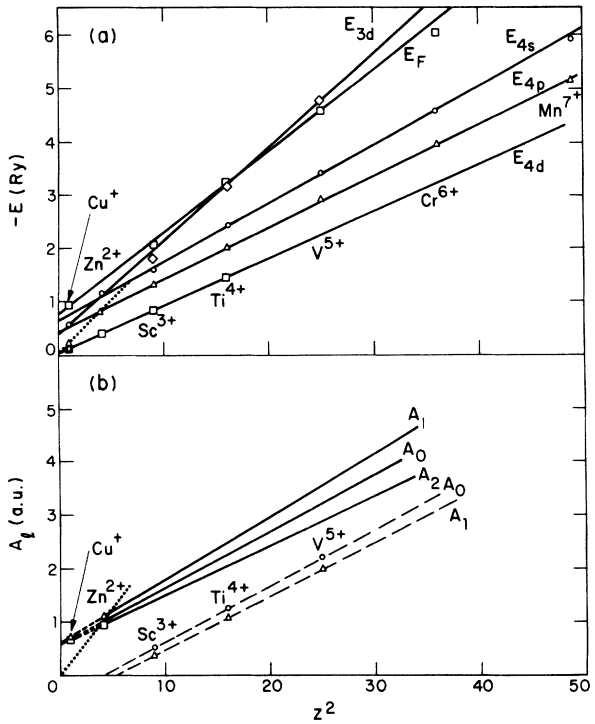

FIG. 4. (a) E_{nl} vs z^2 is the same as in Fig. 1(b), but E_F [see notes Fig. 2(a)] is also shown. Dotted line through origin indicates possible breakdown of Eq. (6) for $z \leq 2$, and a takeover by Eq. (4) (the old quantum-defect relation[6,13]). (b) A_l vs z^2 for the transition-metal sequence of Eq. (3), calculated as in Ref. 8 by linear extrapolation [cf. Fig. 3(a)]. For Sc, A_l vs E_{nl} is *flat*, i.e., the same for all E, and so is independent of uncertainties in determination of E_F [Fig. 4(a)]; thus the discontinuous jump at $z = 2$ is real. The dashed lines are obtained in the same way as for simple metals; the full lines (drawn parallel to the dashed ones) are based on considerations of the Lin-Phillips core shift[16] as discussed in Sec. III.

effect of the core shift is to bring the $3d$ level to the position of the infinity in A_2.

This means that A_2 depends rather strongly on $\mathcal{E}$,

$$A_2(\mathcal{E}) \propto (\mathcal{E} - \mathcal{E}_{3d})^{-1} \tag{18}$$

in the neighborhood of the $3d$ level. Figure 3(b) shows that this form of A_2 is practically independent of the model radius R_m over the entire range of values $2.0 \leq R_m \leq 15.0$ considered in Abarenkov's tables. In addition, because of the scaling property in Eq. (11), which shows that A_l/z^2 is a universal function of $\mathcal{E}/z^2$ for any z, the *resonance* form in Eq. (18) will occur at the same equivalent position for all elements of the $3d$ isoelectronic sequence. Thus, Eq. (18) provides an empirical evidence for the resonance model[19] of transition-metal d bands in the framework of the pseudopotential theory.[10] A more formal characterization

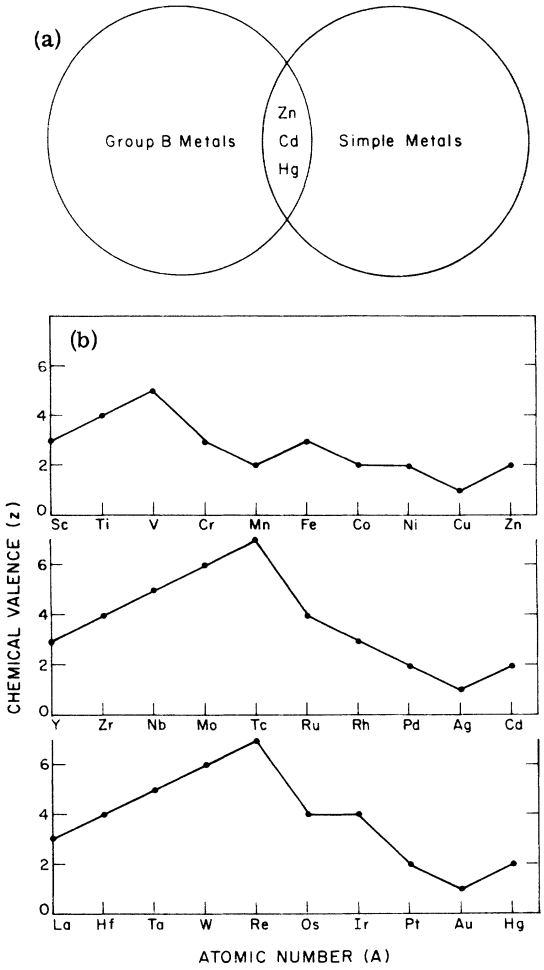

FIG. 5. (a) Illustration of the principle of analytical continuation of model-potential parameters A_l, as functions of the chemical valence z in an isoelectronic sequence, from simple metals (including Zn, Cd, and Hg), to group B (mostly transition metals) (also including Zn, Cd, and Hg). (b) Chemical valence (z) of transition-metal ions used in Table I, as function of the atomic number (A).

of the resonance will be presented in Paper III.

Finally, we turn to the difficult question of *extrapolating* the $A_l(\mathcal{E})$ to the energy $\mathcal{E}_F$ of the electron at the Fermi level in a crystal. First, we use the actual E rather than $\mathcal{E}$, as in Ref. 8. The procedure adopted in Ref. 8 is illustrated by the straight lines joining the three actual s levels, E_{4s}, E_{5s}, and E_{6s} in Fig. 3(a), i.e., the term values lie on a *linear* A_l-vs-E curve at the term values $E = E_{nl}$. From such a straight line, A_l can be obtained at any neighboring energy, in particular E_F. The result of carrying our this procedure using the *actual* spectroscopic term values of the transition metals (instead of the shifted energies, $\mathcal{E}_{nl}$) is illustrated in Fig. 4. The spectroscopic data, together with E_F [calculated as in nontransition metals, from Eq. (23) of Ref. 4] are shown in Fig. 4(a), while the A_l vs z^2 for the sequence of Eq. (3) (at E_F and approximately the same R_m of Table I) are shown in Fig. 4(b) (dashed line). The A_l vs z^2 shows a discontinuity at $z = 2$ (independent of the choice of R_m).

The discontinuity at $z = 2$ is a new feature peculiar to the transition metals which has provided a clue to the physical significance of the "atomic-core shift" Δ in the determination of the TMMP parameters A_l. From Eq. (16), it is clear that the *slope* of A_l vs z^2 can be chosen to be independent of R_m, while the *intercept* on the A_l axis depends on the choice of R_m and therefore reflects the inherent arbitrariness of the pseudopotential: the *intercept* may therefore be interpreted as an analog of the Lin-Phillips *core shift*.[16] Thus, the key distinction between the transition- and simple-metal model-potential theories is provided by the size of the core shift; and a parallel displacement of A_l vs z^2 (dashed line) for $z > 2$, so as to eliminate the discontinuity at $z = 2$ is tantamount to using the same core shift for all group-B metals of the $3d$ series in Fig. 4(b) (solid line): it guarantees that the parameters for Zn (considered as a simple

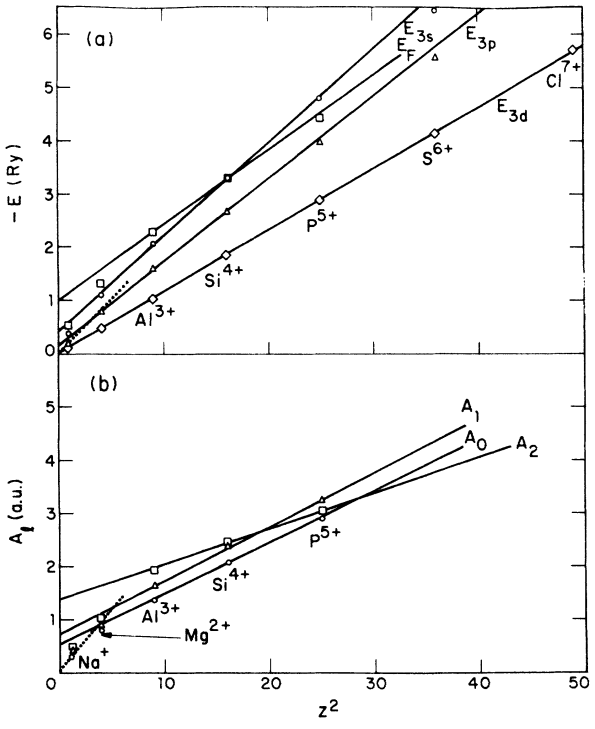

FIG. 6. (a) E_{nl} vs z^2 for the group-A elements of the third row; observe breakdown of Eq. (6) for $z < 2$, as in Fig. 4(a). (b) A_l vs z^2 for the following values of R_m; 3.4 for Na, 2.6 for Mg, 2.0 for Al, Si, and P at E_F. Parameters are taken directly from Ref. 4 (Table 4).

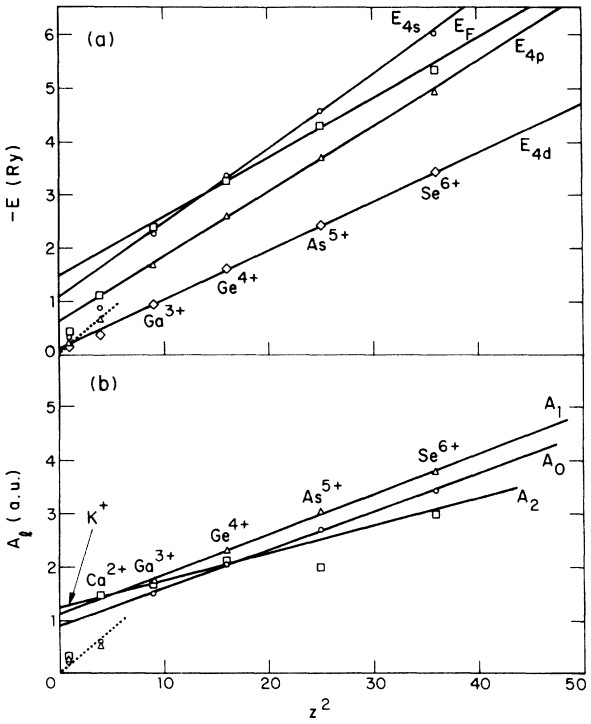

FIG. 7. (a) E_{nl} vs z^2 for the group-A elements of the fourth row. (b) A_l vs z^2 for the following values of R_m: 4.2 for K, 2.6 for Ca, 2.0 for Ga, Ge, As, and Se, from Ref. 4 (Table 4) (except Ga, which has been recalculated at $R_m = 2.0$, in order to exhibit the effect of keeping R_m the same for $z \geq 3$).

metal) is the same as the TMMP parameters for Zn [considered as a group-B (transition) metal]. Accordingly, Zn, Cd, and Hg provide a basis for relating TMMP and simple-metal model-potential parameters [Fig. 5(a)] in the respective $3d$, $4d$, and $5d$ series. On the other hand, a discontinuous slope of A_l vs z^2 at $z = 2$ can be expected, inasmuch as the old quantum-defect concept works for group-I and -II elements, i.e., it is possible to find quantum defects ($\delta'_{nl} \neq 0$, $\Delta'_{nl} = 0$) such that E_{nl} vs z^2 passes through the origin [see dotted line in Fig. 4(a)], and similarly A_l vs z^2 passes through the origin [see dotted line in Fig. 4(b)].

We now summarize these observations, as a recipe for extrapolating the A_l to neighboring energies in the spirit of the QDM, and generating A_l vs z^2 in an isoelectronic sequence of transition metals.

(i) The *slope* of A_l vs z^2 for an isoelectronic sequence is determined as for simple metals by Abarenkov's tables [cf. Fig. 3(a)], but the energy parameter to which TMMP parameters refer is $\mathcal{E} = E - \Delta$.

(ii) The intercept of A_l vs z^2 on A_l axis is determined by treating Zn, Cd, and Hg as both simple metals[4,18] and transition metals [see Fig. 5(a)], and the R_m's may be varied within $R_c \lesssim R_m < R_a$, over which range we expect A_l vs z^2 to be *linear*, just as in simple metals.

(iii) The slope of A_l vs z^2 ($z \geq 2$) may be determined when spectroscopic data are not available by comparing elements of the same *column* (i.e., same chemical valence) in the Periodic Table; for $z \leq 2$, the validity of the old quantum-defect concept suggests that A_l vs z^2 may pass through the origin [as indicated by the dotted line in Fig. 4(b)].

(iv) The *effective valence* (z) of a transition-metal ion in the crystal [Fig. 5(b)] is given by the *nominal* value for elements with completely full or less than half-full d shells; e.g., $z = 4$ for Ti (group IVB); but is determined for all others, e.g., $z = 3$ for Fe (group VIII), mostly by the stability of the *half-full d shell*, as suggested by the commonest chemical compounds of the transition metal.

The essence of the above recipe lies in the successful application of the TMMP method (in the simplest possible way, preferably in local TMMP approximation) to the calculation of solid-state properties, e.g., the phonon spectra of Paper II. It applies in the same way to simple and transition metals.

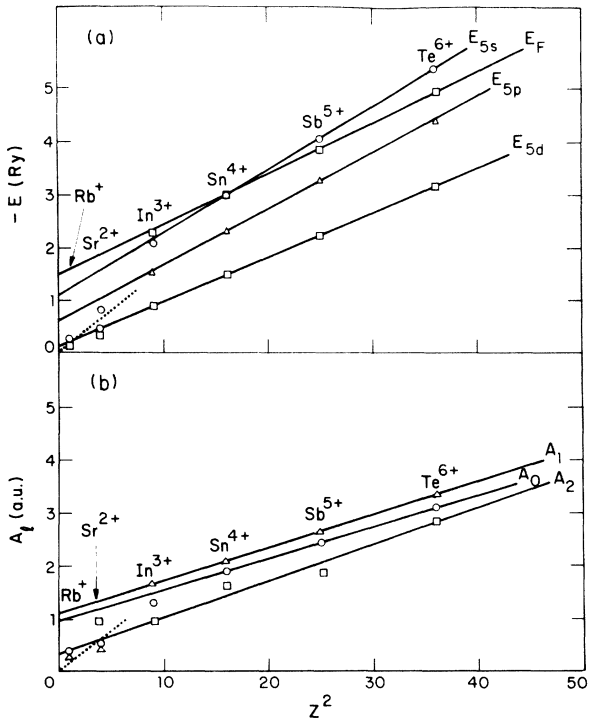

FIG. 8. (a) E_{nl} vs z^2 for the group-A elements of the fifth row. (b) A_l vs z^2 for the following values of R_m: 4.4 for Rb, 3.6 for Sr (Ref. 18 Table 1), 2.4 for In, and 2.0 for Sn, Sb, and Te, from Ref. 4 (Table 4).

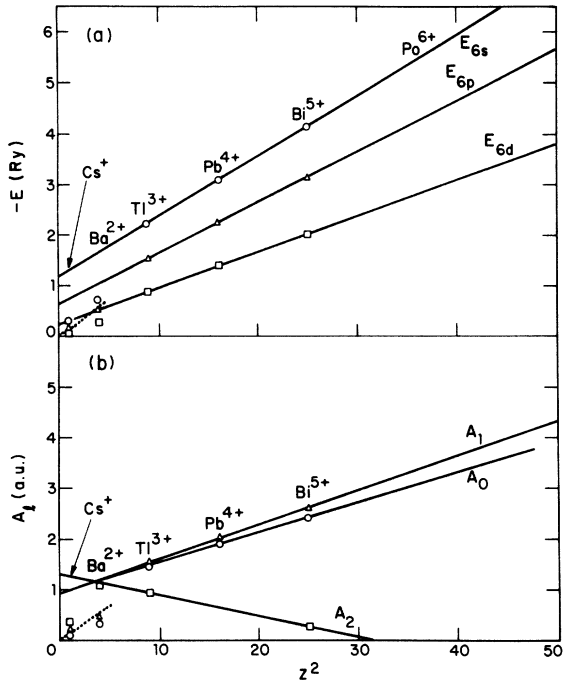

FIG. 9. (a) E_{nl} vs z^2 for the group-A elements of the sixth row. (b) A_l vs z^2 for the following values of R_m, 4.8 for Cs, 3.6 for Ba (Ref. 18 Table 1), 2.4 for Tl, 2.1 for Pb, and 2.0 for Bi, from Ref. 4 (Table 4).

IV. NUMERICAL RESULTS AND DISCUSSION

In this section we shall verify the generalized quantum-defect law (6) as well as the associated linearity of the model-potential parameters A_l (as function of z^2 in an isoelectronic sequence) for the remaining group A and B elements of the Periodic Table; the parameters of the TMMP appropriate for a valence electron at the Fermi level in the crystal will be tabulated; the calculation of the TMMP form factors will be discussed in the simplest (local) screening approximation; and the results will be discussed.

Figures 6(a) and 6(b)–9(a) and 9(b) cover the remaining group-A elements of the third, fourth, fifth, and sixth row. These figures show that Eq. (6) is quite well obeyed by all group-A positive ions, and that A_l vs z^2 is linear (especially for $z \geq 2$) over a range of R_m's in $R_c \lesssim R_m < R_a$.

Figures 10(a) and 10(b) and Figs. 11(a) and 11(b) apply to the remaining group-B transition-metal sequences Ag^+, Cd^{2+}, Y^{3+}, ..., Pd^{10+} (fifth row), and Au^+, Hg^{2+}, La^{3+}, ..., Pt^{10+} (sixth row). The spectroscopic data for these metals are scanty, [5] but except for the sixth row we always had enough term values to determine the slope of E_{nl} vs z^2 and of A_l vs z^2 with adequate accuracy, for $l = 0$, 1, but not for A_2.

From these graphs we have interpolated the parameters of the TMMP at given values of the chemical valence z for the pertinent model radii, R_m. The results are tabulated in Table I, and apply to a valence electron at the Fermi level in the solid. Our expectation is that these parameters will simply be plugged into the usual expression for the simple-metal model-potential form factors $V(q)$, given by Animalu and Heine. [4] However, because of the strong energy dependence of A_2, which, as pointed out in Eq. (18) above, is related to s-d hybridization in the transition metals, the pertinent form of the TMMP [incorporating the usual approximation, $A_l = C$ $(l \geq 3)$] is

$$V_m(r) = -C - (A_0 - C)P_0 - (A_1 - C)P_1 - (A_2 - C)P_2 \quad \text{for } r \leq R_m$$
$$= -z/r \quad \text{for } r > R_m, \qquad (19)$$

where, specifically, $C = z/R_m$ is quite adequate for phonon-spectrum calculation (Paper II).

In view of Eq. (18), the potential

$$V_{rs}(r) = -(A_2 - C)P_2 \quad \text{for } r \leq R_m$$
$$= 0 \quad \text{for } r > R_m, \qquad (20)$$

corresponds to Harrison's hybridization or reso-

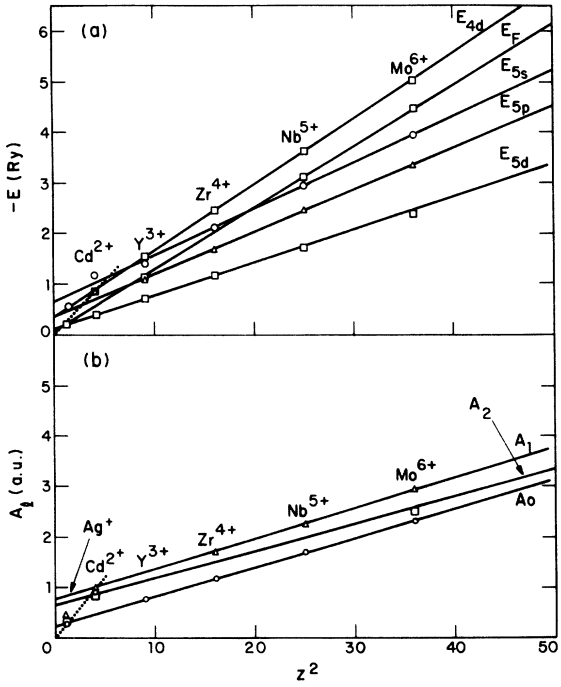

FIG. 10. (a) E_{nl} vs z^2 for the group-B elements of the fifth row. (b) A_l vs z^2, at the R_m's of Table I. Both spectroscopic data and phonon spectrum (Ref. 1) were taken into account in the determination of the linear trajectory. Note that the spectroscopic data are scanty, especially for the d levels (see Ref. 5).

nance term: it is a rapidly varying function of the energy. Apart from this strong energy dependence, V_{rs} is of the same form as the Fong-Cohen empirical (d-partial-wave) model potential.[20]

The full TMMP for a bare ion is $V_m + V_{oc} + V_{cc} = V^b$ say, where V_{oc} and V_{cc} are, respectively, the usual orthogonalization and correlation corrections.[4] For definiteness, the analytical expression for the screened-model-potential form factor, $V(q) = V^b(q)/\epsilon(q)$, $\epsilon(q)$ being the dielectric function of the electron gas, in local screening approximation, is displayed in Appendix A below. Numerical results for Zn in the usual (simple-metal) approximation ($C \equiv A_2$) and in the TMMP approximation ($C = z/R_m \neq A_2$) are displayed in Fig. 12.

It should be observed in Fig. 12 that the resonance term is more important in the region $q \gtrsim 2k_F$; Harrison[10] found the resonance term more important in the small q region, $q < 2k_F$. The former is easier to understand physically, for if the resonance term is to transcend the tight-binding character of the d-shell electrons, then the Fourier transform of the potential associated with it should

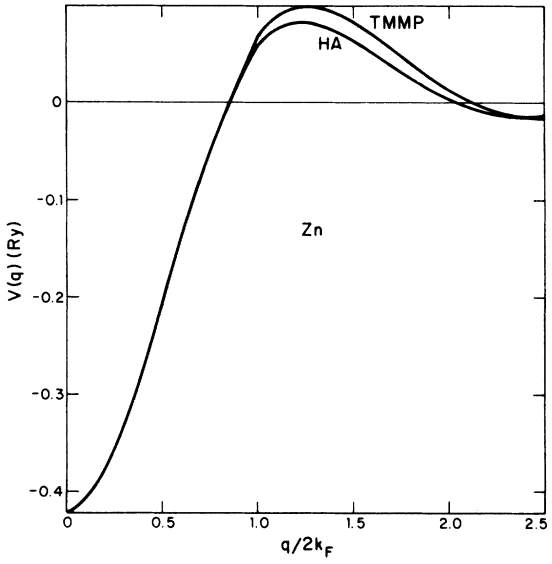

FIG. 12. $V(q)$ in Heine-Abarenkov approximation $C = A_2$ in Eq. (19) is compared with the transition-metal model potential (TMMP) (in the approximation $C = z/R_m \neq A_2$).

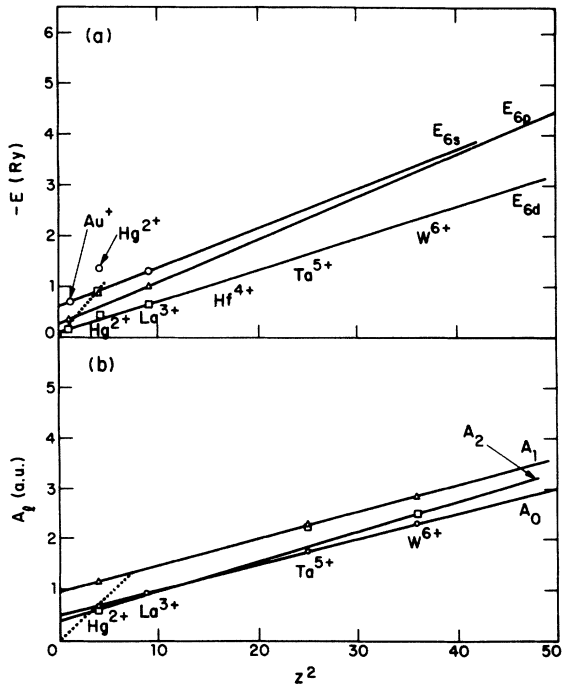

FIG. 11. (a) E_{nl} vs z^2 for the sixth row group-B elements (excluding the rare-earths, for which the appropriate spectroscopic data[5] are lacking). Only the spectroscopic data for Au, Hg, and La are available for the ionized states of interest in this sequence, and these are somewhat erratic (as the experimental points indicate). (b) A_l vs z^2, at the R_m's of Table I, obtained from consideration of the systematics of spectroscopic data along rows and columns of the Periodic Table and from phonon spectrum (Ref. 1).

be appreciable at large q (corresponding in real space to a potential that is strong at small distances from the center of the ion core). More $V(q)$'s will be included in Paper II. The calculation is straightforward, at least in the simple screening approximation presented in Appendix A.

Finally, in pursuit of the dependence of spectroscopic data on the chemical valence, we show in Fig. 13 a suggestive correlation[21] of the superconducting transition temperature T_c and the square

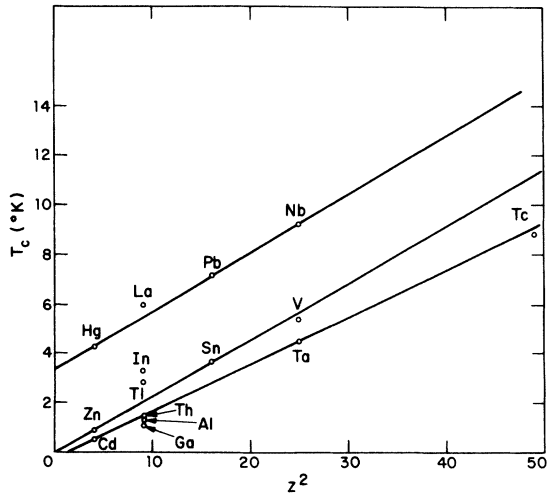

FIG. 13. Empirical correlation between T_c (the superconducting transition temperature) and z^2. Experimental data have been taken from Kittel (Ref. 12, p. 402) except for technetium (taken from Matthias, Ref. 21).

(z^2) of the chemical valence, for pure crystalline metals of the Periodic Table: one can attempt to explain this systematics in terms of the scaling property of the atomic pseudopotential determining the strength of the electron-phonon interaction for elements belonging to an isoelectronic sequence; but we shall not pursue the analysis here.

V. CONCLUSIONS

We have shown in this paper, by unscrambling the atomic-spectroscopic data in terms of the empirical relation of Eq. (6), that the notion of quantum defects applies to all elements of the first six rows of the Periodic Table. For groups I*A* and I*B*, and II*A* and II*B*, ordinary and transition metals, it appears that the old quantum-defect concept of Eq. (4) applies quite well, but for elements of groups III*A* and III*B*, etc., Eq. (6) including the *new quantum defect* Δ_{nl} (which we have interpreted as a "core shift") is clearly a better representation of reality. The most important property of the quantum defects for both simple and transition metals is the *universality* for elements of one inert-gas configuration, i.e., for an isoelectronic sequence: This property provides a basis for a *universal model potential* theory of positive ions of all elements of the Periodic Table. The Fermi energy E_F of an electron relative to a positive ion (as formulated by Animalu and Heine[4]) also shares this property and justifies the extension of the quantum-defect concept to the solid.

The model-potential parameters given in Table I for the transition metals will undoubtedly be as useful as the parameters for the simple metals, published earlier by Animalu and Heine.[4] In deciding the best way to generate these parameters, extensive calculation of the various aspects of the electronic structure of the transition metals, such as phonon spectra, liquid metal resistivity, and energy bands, have been performed in local pseudopotential approximation, using our old programs for simple metals. Interesting systematics have been observed and will be reported in subsequent articles of this series. At each level, we find that the model-potential approach leads to reasonable agreement between theory and experiment.

TABLE I. Parameters of the transition-metal model potential. All quantities are in atomic units except $|E_c|$, which is in rydberg; Ω and R_c have been taken from Kittel's book (Ref. 12, p. 38) and the General Electric x-ray periodic chart, respectively; and the parameters A_l apply to $E=E_F$ and have been interpolated from Figs. 4(b), 10(b), and 11(b).

	A_0	A_1	A_2	R_m	Ω	z	m^*	R_c	α_{eff}	$\lvert E_c \rvert$
Cu	0.25	0.40	0.215	2.2	79.4	1	1.0	1.814	0.157	0.086
Ag	0.223	0.40	0.218	2.6	115.4	1	1.0	2.381	0.245	0.082
Au	0.15	0.50	0.212	2.6	114.6	1	1.0	2.589	0.317	0.082
Zn	0.99	1.14	0.98	2.2	102.0	2	1.1	1.570	0.079	0.091
Cd	0.89	0.98	0.87	2.6	144.8	2	1.0	1.950	0.107	0.087
Hg	0.97	1.11	0.85	2.6	157.8	2	1.0	2.120	0.126	0.086
Sc	1.60	1.65	1.40	2.0	168.7	3	1.0	1.531	0.045	0.090
Y	0.75	1.30	1.10	2.0	223.1	3	1.0	1.739	0.049	0.087
La	0.90	1.40	0.85	2.0	252.2	3	1.0	2.154	0.083	0.086
Ti	2.30	2.50	2.10	2.0	119.0	4	1.0	1.285	0.037	0.096
Zr	1.15	1.70	1.50	2.0	157.0	4	1.0	1.493	0.044	0.095
Hf	1.30	1.80	1.35	2.0	150.2	4	1.0	1.474	0.045	0.095
V	3.25	3.50	2.90	1.6	93.9	5	1.0	1.115	0.031	0.101
Nb	1.70	2.30	2.25	2.0	121.3	5	1.0	1.304	0.038	0.100
Ta	1.75	2.35	2.25	2.0	121.3	5	1.0	1.285	0.038	0.100
Cr	1.60	1.47	1.40	2.5	80.6	3	1.0	1.191	0.044	0.102
Mo	2.30	2.93	2.50	2.0	105.5	6	1.0	1.323	0.046	0.100
W	2.30	2.85	2.50	2.0	106.5	6	1.0	1.172	0.032	0.101
Mn	0.89	0.98	0.87	2.2	81.9	2	1.0	1.512	0.088	0.095
Tc	3.10	3.20	3.30	2.0	96.5	7	1.0	1.058	0.026	0.102
Re	2.95	3.55	3.30	2.0	99.3	7	1.0	1.058	0.025	0.102
Fe	1.60	1.65	1.40	2.0	79.8	3	1.0	1.400	0.072	0.090
Ru	1.15	1.70	1.50	2.0	91.9	4	1.0	1.266	0.046	0.098
Os	1.30	1.80	1.35	2.0	94.8	4	1.0	1.304	0.049	0.098
Co	0.99	1.05	0.98	2.2	74.9	2	1.0	1.360	0.070	0.094
Rh	0.75	1.30	1.10	2.0	92.6	3	1.0	1.285	0.048	0.096
Ir	1.30	1.80	1.35	2.0	95.5	4	1.0	1.285	0.047	0.098
Ni	0.99	1.05	0.98	2.2	73.6	2	1.0	1.304	0.063	0.093
Pd	0.89	0.75	0.87	2.6	99.3	2	1.0	1.512	0.073	0.091
Pt	0.97	1.11	0.85	2.6	101.6	2	1.0	1.512	0.071	0.091

ACKNOWLEDGMENTS

I wish to thank Dr. G. F. Dresselhaus for helpful comments and suggestions, Professor Walter A. Harrison for a valuable correspondence, Professors H. Ehrenreich and F. S. Ham for fruitful discussions, and Dr. H. J. Zeiger for his interest and encouragement. Most of the graphical display of results and the consequent insight would have been impossible but for the assistance of Miss Susan Landon in computer programming, which is hereby gratefully acknowledged.

APPENDIX A

In this Appendix, we wish to give an explicit expression for the screened-model-potential form factor $V(q)$. In the local screening approximation

$$V(q) = V^b(q)/\epsilon(q), \tag{A1}$$

where

$$V^b(q) = \langle \vec{k}_F + \vec{q} | (V_m + V_{oc} + V_{cc}) | \vec{k}_F \rangle \equiv F(\vec{k}_F, \vec{k}_F + \vec{q}) + B(q) \tag{A2}$$

say, V_m being the model potential defined by Eq. (19) and V_{oc}, V_{cc} the usual orthogonalization and correlation corrections of Ref. 4.

In Eq. (A2),

$$B(q) = -\frac{8\pi C}{\Omega q^3}[\sin(qR_m) - qR_m\cos(qR_m)] - \frac{8\pi z}{\Omega q^2}\cos(qR_m) + \left(\frac{4\pi|E_c|}{\Omega q^3} - \frac{24\pi z\alpha_{eff}}{\Omega q^2(qR_c)^3}\right) \times [\sin(qR_c) - qR_c\cos(qR_c)]. \tag{A3}$$

For $|\vec{k}_F + \vec{q}| = k_F$,

$$F(\vec{k}_F, \vec{k}_F + \vec{q}) = -4\pi\Omega^{-1}R_m^3(A_0 - C)\{[j_0(x)]^2 - x^{-1}\cos(x)j_1(x)\} - 12\pi\Omega^{-1}R_m^3(A_1 - C) \times \{[j_1(x)]^2 - j_0(x)j_2(x)\}P_1(\cos\theta) - 20\pi\Omega^{-1}R_m^3(A_2 - C)\{[j_2(x)]^2 - j_1(x)j_3(x)\}P_2(\cos\theta), \tag{A4}$$

where $x = k_F R_m$, $\cos\theta = (1 - q^2/2k_F^2)$;

$P_1(\cos\theta) = \cos\theta$, $P_2(\cos\theta) = \frac{1}{2}(3\cos^2\theta - 1)$;

$j_0(x) = x^{-1}\sin x$, $j_1(x) = x^{-2}\sin x - x^{-1}\cos x$, $j_2(x) = (3x^{-3} - x^{-1})\sin x - 3x^{-2}\cos x$, $j_3(x) = 5x^{-1}j_2(x) - j_1(x)$.

For $|\vec{k}_F + \vec{q}| \neq k_F$,

$$F(k_F, k_F + q) = -\frac{8\pi R_m^3(A_0 - C)}{\Omega(x^2 - y^2)}[xj_1(x)j_0(y) - yj_1(y)j_0(x)] - \frac{24\pi R_m^3(A_1 - C)}{\Omega(x^2 - y^2)} \times [xj_2(x)j_1(y) - yj_2(y)j_1(x)]P_1(\cos\theta') - \frac{40\pi R_m^3(A_2 - C)}{(x^2 - y^2)}[xj_3(x)j_2(y) - yj_3(y)j_2(x)]P_2(\cos\theta'), \tag{A5}$$

where

$$x = k_F R_m, \quad y = |\vec{k}_F + \vec{q}|R_m, \quad \cos\theta' = [x^2 + y^2 - (qR_m)^2]/2xy. \tag{A6}$$

The dielectric function $\epsilon(q)$ is given by

$$\epsilon(q) = 1 + [1 - f(q)](4\pi z e^{*2}/\Omega q^2)\chi(q/2k_F), \tag{A7}$$

where

$$\chi(X) = (3E_F/2)\left[\frac{1}{2} + \frac{1}{4}\left(\frac{1 - X^2}{X}\right)\ln\left|\frac{1 + X}{1 - X}\right|\right], \tag{A8}$$

$$E_F = (\hbar^2 k_F^2/2m^*), \tag{A9}$$

$$e^{*2} = (1 + \alpha_{eff})e^2, \tag{A10}$$

and

$$f(q) = q^2/[2(q^2 + k_F^2 + k_s^2)]; \quad k_s^2 = 2k_F/\pi \text{ (a.u.)}. \tag{A11}$$

In the TMMP of Fig. 12 for Zn, the approximation

$$C = z/R_m \tag{A12}$$

was used, together with Table I, in evaluating $V(q)$. The final answer obtained by inserting the numbers in Table I into $V(q)$ is in Ry.

*Work sponsored by the U.S. Air Force.

[1] A. O. E. Animalu, following paper, Phys. Rev. B **8**, 3555 (1973); Phys. Rev. B. (to be published).
[2] I. V. Abarenkov and V. Heine, Philos. Mag. **12**, 529 (1965).
[3] V. Heine and I. V. Abarenkov, Philos. Mag. **9**, 451 (1964).
[4] A. O. E. Animalu and V. Heine, Philos. Mag. **12**, 1249 (1965).
[5] C. E. Moore, *Atomic Energy Levels* (National Bureau of Standards, Washington, D.C., 1949), Vols. I, II, and III.
[6] F. S. Ham, Solid State Phys. **1**, 127 (1955).
[7] R. Jacobs, J. Phys. C **1**, 1296 (1968); J. Phys. C **1**, 1307 (1968).
[8] A. O. E. Animalu, Technical Report No. 4, Solid State Theory Group, Cavendish Laboratory, Cambridge, England, 1965 (unpublished).
[9] R. W. Shaw, Jr., Phys. Rev. **174**, 769 (1968); Ph.D. thesis (Stanford University, 1968) (unpublished).
[10] W. A. Harrison, Phys. Rev. **181**, 1036 (1969).
[11] L. Hodges, R. E. Watson, and H. Ehrenreich, Phys. Rev. B **5**, 3953 (1972).

[12]General Electric X-Ray Period Chart; C. Kittel, *Introduction to Solid State Physics* (Wiley, New York, 1971), 4th ed., p. 129.
[13]M. J. Seaton, Proc. Phys. Soc. Lond. **88,** 801 (1966); Proc. Phys. Soc. Lond. **88,** 815 (1966); Proc. Phys. Soc. Lond. **88,** 833 (1966); Proc. Phys. Soc. Lond. **88,** 843 (1966).
[14]D. R. Hartree, Proc. Cambridge Phil. Soc. **24**, 89 (1927); Proc. Cambridge Phil Soc. **24**, 111 (1927); Proc. Cambridge Phil. Soc. **24**, 426 (1927); Proc. Cambridge Phil. Soc. **25**, 310 (1929).
[15]I. S. Bowen and R. A. Millikan, Phys. Rev. **24,** 209 (1924); see also, A. C. Candler, *Atomic Spectra and the Vector Model* (Cambridge U.P., Cambridge, England, 1937), Chap. XI.
[16]P. J. Lin and J. C. Phillips, Adv. Phys. **14,** 257 (1965).
[17]M. Blume, N. Briggs, and H. Brooks, Tables of Coulomb Functions, Tech. Rept. No. 126, (Cruft Laboratory, Harvard University, 1959) (unpublished).
[18]A. O. E. Animalu, Proc. R. Soc. A **294,** 376 (1966).
[19]J. M. Ziman, Proc. Phys. Soc. Lond. **86**, 337 (1965); V. Heine, Phys. Rev. **153,** 673 (1967); J. Hubbard, Proc. Phys. Soc. Lond. **92,** 921 (1967).
[20]C. Y. Fong and M. L. Cohen, Phys. Rev. B **6,** 3633 (1972).
[21]B. T. Matthias, Physics Today **24** (8), 23 (1971).